

DEVELOPMENT OF TSUNAMI FORECAST MODEL FOR FLORENCE, OREGON

Dylan Righi

September 30, 2009

Contents

Abstract.....	6
1.0 Background and Objectives	6
2.0 Forecast Methodology.....	7
2.1 Study Area – context	7
2.2 Tide Gauge data	7
2.3 Historical events	7
2.4 Bathymetry and Topography	7
2.5 Model Setup.....	8
3.0 Results.....	8
3.1 Model Validation	8
3.2 Model stability and reliability	9
4.0 Summary and Conclusions.....	9
5.0 Acknowledgments.....	10
6.0 References	10
7.0 Appendix A.....	10
7.1 RIM *.infile for Port Orford, Oregon.....	10
7.2 SIM *.infile for Port Orford, Oregon	11

List of Tables

Table 1 NGDC run up observations for Port Orford	13
Table 2 MOST Model set up parameters for Port Orford, Oregon.....	14
Table 3 Tsunami sources of 11 historical events used for model validation in this study.	15
Table 4. Unit source combinations used for the 16 artificial mega-events.....	17

List of Figures

Figure 1 Evacuation map for Port Orford, Oregon developed by the Oregon Department of Geology and Mineral Industries in consultation with local officials. It is intended to represent a worst-case scenario for a tsunami caused by an undersea earthquake near the Oregon coast. Evacuation routes were developed by local officials and reviewed by the Oregon Department of Emergency Management.....18

Figure 2 Google Maps image of Port Orford. The yellow arrow indicates the approximate location of the Port Orford tide gauge.....19

Figure 3 Bathymetry (in meters) for the Port Orford RIM grids. The A grid is shown in the top left axis, the B grid in the bottom left, and the C grid on the right. The land topography of the C grid is shown using contours with 25 meter intervals. The red boxes in the A and B plots show the position of the B and C grids, respectively.20

Figure 4 Bathymetry (in meters) for the Port Orford RIM grids. The A grid is shown in the top left axis, the B grid in the bottom left, and the C grid on the right. The land topography of the C grid is shown using contours with 25 meter intervals. The red boxes in the A and B plots show the position of the B and C grids, respectively.21

Figure 5 Model results for the 1946 Unimak event. Top left and right axes show, respectively, the SIM and RIM maximum wave height results. The lower axis shows the model wave heights at the geographical position of the Port Orford tide gauge.22

Figure 6 Model results for the 1994 Kuril event. Top left and right axes show, respectively, the SIM and RIM maximum wave height results. The lower axis shows the model and data wave heights at the Port Orford tide gauge.....23

Figure 7 Model results for the 1996 Andreanof event. Top left and right axes show, respectively, the SIM and RIM maximum wave height results. The lower axis shows the model and data wave heights at the Port Orford tide gauge.....24

Figure 8 Model results for the 2001 Peru event. Top left and right axes show, respectively, the SIM and RIM maximum wave height results. The lower axis shows the model wave heights at the geographical position of the Port Orford tide gauge.25

Figure 9 Model results for the 2003 Rat Island event. Top left and right axes show, respectively, the SIM and RIM maximum wave height results. The lower axis shows the model wave heights at the geographical position of the Port Orford tide gauge.26

Figure 10 Model results for the 2006 Tonga event. Top left and right axes show, respectively, the SIM and RIM maximum wave height results. The lower axis shows the model wave heights at the geographical position of the Port Orford tide gauge.27

Figure 11 Model results for the 2006 Kuril event. Top left and right axes show, respectively, the SIM and RIM maximum wave height results. The lower axis shows the model and data wave heights at the Port Orford tide gauge.....28

Figure 12 Model results for the 2007 Kuril event. Top left and right axes show, respectively, the SIM and RIM maximum wave height results. The lower axis shows the model wave heights at the geographical position of the Port Orford tide gauge.29

Figure 13 Model results for the 2007 Solomon Islands event. Top left and right axes show, respectively, the SIM and RIM maximum wave height results. The lower axis shows the model wave heights at the geographical position of the Port Orford tide gauge.30

Figure 14 Model results for the 2007 Peru event. Top left and right axes show, respectively, the SIM and RIM maximum wave height results. The lower axis shows the model wave heights at the geographical position of the Port Orford tide gauge.31

Figure 15 Model results for the 2007 Chile event. Top left and right axes show, respectively, the SIM and RIM maximum wave height results. The lower axis shows the model wave heights at the geographical position of the Port Orford tide gauge.32

Figure 16 Wave heights (in meters) from the SIM model at the location of the Port Orford tide gauge for 16 hypothetical mega-tsunami scenarios. The x-axis units are hours since the event earthquake.33

Development of a Tsunami Forecast Model for Florence, Oregon

Dylan Righi

Abstract

The Short-term Inundation Forecasting for Tsunamis (SIFT) system is under development by the NOAA Center for Tsunami Research (NCTR) at the Pacific Marine Environmental Laboratory (PMEL) to provide Tsunami Warning Centers (TWCs) with a capability to produce efficient forecasts for tsunami arrival time, heights and inundation for the target coastlines given a tsunami event. The development of Standby Inundation Model for Florence, Oregon is described as a component of the SIFT system. The optimized SIM can provide a 4-hour local forecast of first wave arrival, amplitudes and reasonable inundation limit in minutes. It shows robust results for all historical validation and stability test cases.

1.0 Background and Objectives

An efficient tsunami forecast system provides timely basin-wide warning of in-progress tsunami waves accurately and quickly (Titov et al., 2005). NOAA's Short-term Inundation Forecast of Tsunami (SIFT) is an advanced tsunami forecasting system that combines real-time tsunami event data with numerical models to produce estimates of tsunami wave arrival times and amplitudes. The SIFT system integrates several key components: the tsunameters for real-time monitoring of tsunami signals in the deep ocean, a basin-wide pre-computed propagation database of water level and flow velocities based on potential seismic unit sources, an inversion algorithm to derive the tsunami source based on the tsunameter observations during a tsunami event, and the Stand-by Inundation Models (SIMs) to provide accurate and speedy numerical modeling of tsunami impact for coastal communities. A SIM is used to create the forecast model to provide an estimate of wave arrival time, wave height, and inundation immediately after a tsunami event. Tsunami forecast models are run in real time while a tsunami is propagating in the open ocean; consequently they are designed to perform under very stringent time limitations. The Stand-by Inundation Model (SIM), based on the Method of Splitting Tsunami (MOST), emerges as the solution in SIFT by modeling real-time tsunami in minutes while employing high-resolution grids. Each SIM consists of three telescoped grids with increasing spatial resolution, and temporal resolution for simulation of wave inundation onto dry land.

The SIM utilizes the most recent bathymetry and topography available to reproduce the correct wave dynamics during the inundation computation. SIMs are constructed for populous coastal communities at risk for tsunamis in the Pacific, Atlantic and Caribbean. Previous and present development of SIM in the Pacific (Titov et al., 2005; Titov, 2009; Tang et al., 2008; Wei et al., 2008) has shown the accuracy and efficiency of the up-to-date SIMs implemented in SIFT in the real-time tsunami forecast, as well as in hindcast research.

The objective of SIM development is to provide real-time tsunami predictions for selected coastal locations while the tsunami is propagating through the open ocean, before the waves have reached many coastlines. SIMs will be incorporated into the U.S. tsunami warning system for use at the Pacific and West Coast-Alaska Tsunami Warning Center. Titov and Gonzalez (1997) and Tang et al (2008) describe the technical aspects of SIM development, stability testing and robustness.

Florence Oregon is located on the central Oregon coast, where the Siuslaw River meets the ocean. According to the 2000 U.S. Census, the population of Florence was 7263, a 40.7% increase from the 1990 U.S. Census. The cities current economy is based on tourism and retirement, a change from a past natural resource oriented economy (logging, fishing and agriculture). Florence is at the junction of Highways 101 and 126, about 50 miles south of Newport along the coastal Highway 101 and 75 miles to the east of Eugene on Highway 126. Highway 101 crosses the Siuslaw River on the historic Siuslaw River

Bridge, which opened in 1936. Florence is also home Other points of interest for tsunami hazard assessment are Peace Harbor Hospital, a small regional trauma center, the Florence Municipal Airport, and the new Three Rivers Casino and Hotel.

2.0 Forecast Methodology

The methodology for modeling these coastal areas is to develop a set of three nested grids (A, B, C), each of which is successively finer in resolution, until the near-shore details can be resolved to the point that tide gauge data from historical tsunamis in the area match reasonably with the modeled results. The procedure is to start with large spatial extent merged bathymetric topographic grids at high resolution, referred to as a "reference SIM" (RIM), and then after a reasonable data fit is achieved to optimize these grids by coarsening the resolution and shrinking the grid size until the model runs in under 10 min of wall-clock time. This allows for the significant portion of the modeled tsunami waves, typically 4 to 10 hr of modeled tsunami time, to pass through the model domain without too much signal degradation. This final model is referred to as the "optimized SIM".

2.1 Study Area – context

Florence is on the Siuslaw River with almost all of the population living to the north of the river.

2.2 Tide Gauge data

There is no tide gauge available for model validation of the Florence forecast model.

2.3 Historical events

2.4 Bathymetry and Topography

Accurate bathymetry and topography are crucial inputs to developing the reference and standby models, especially for the inundation of the near-shore environment. To develop each grid, we attempt to gather and use the best available data for the area studied. Grids may be updated if newer, more accurate data are available. For the development of the Florence grids, a 1/3-arc-sec merged bathymetric and topographic digital elevation model was developed by NGDC for tsunami inundation modeling. To increase the size of the grids to encompass the larger B grid and the regional A grid, a 6-sec Oregon coast grid and a 36-sec Pacific Northwest grid were combined, resampled, and error checked to extend the domain for the grid extents. Grids are made available in the ESRI ArcGIS raster format. Additionally, all data were converted to the WGS 84 vertical datum.

Final grids used for the reference and standby models are described in Table 2 and Figs. 3 and 4. Each set of grids is nested with increasing resolution from the larger regional grids to the higher resolution community-based grid. The RIM A grid extent is region wide, covering from central Washington on the northern boundary and south to almost San Francisco Bay in central California at a 36 arc second resolution. The A grid depth reached a maximum of 4350m. The B grid has a resolution of 6 arc-seconds and its extent was reduced to cover most of Oregon and part of northern California. The grid was able to extend to an offshore depth of ~730m. The reference C grid was designed to cover a reasonable distance north and south of the Siuslaw River mouth along the coast and at the same time be able to describe how a wave moves up the river channel to the more populated areas. With grid spacing of 1/3 arc-second,

or ~10 meters, it is the highest resolution grid used. The maximum depth of the C grid is 52m.

The forecast model grids all keep the same extents as the RIM grid, but their resolution is reduced in order to allow the models to be processed faster. The SIM A, B and C resolutions are 72, 12 and 2 arc-seconds respectively. These resolutions allow a time step of 1.2 seconds to be used for the SIM model runs.

2.5 Model Setup

The model used to estimate tsunami amplitude is the MOST model (Titov and González, 1997; Synolakis et al., 2007; Tang et al., 2008), which is a finite difference method of characteristic model which takes input from a propagation-run data base and then, via a series of nested grids, resolves the near-shore bathymetry and topography to estimate the water level at coastal sites. Adjustable parameters include time step, number of time steps, near shore wet/dry boundary depth, coarse grid wet/dry boundary depth, run down or not in coarse grids friction coefficient, output time, grid size, grid resolution, and grid position. Once tested, these parameters remain fixed from run to run, under the assumption that the parameters and features may be location dependent, including sharp bathymetric changes and high-resolution grids needed to resolve for channels, but should not depend on the flow field. For Florence the grid resolution and extents for the reference and optimized (stand-by) grids are given in Table 2. Figures of the model extents for reference and optimized grids are shown in Figs. 3 and 4.

3.0 Results

3.1 Model Validation

Several events were used to test the Florence RIM and tsunami forecast model development. The eleven events used and their time, location and source description are presented in Table 2.

Comparisons of the RIM and forecast model results are shown in Figs. 5 - 15 for the historical events. In each figure, the top left and right panels show, respectively, the forecast model and RIM maximum wave heights (cms). The bottom panels show the wave heights at the A and B locations shown in the forecast model map. The A point is outside and to the south of the river channel breakwaters, and the B point is on the Siuslaw River south of the Florence docks. Note that the color scale and plot limits of the figures change with each event.

The 1946 Unimak event is the largest historical event modeled for this report. The maximum wave heights predicted by the forecast and reference models show similar patterns and magnitudes (Figure 5). The largest wave heights are found south of the breakwater in both models and reach ~60 cms. The waves that progress up the Siuslaw River are smaller. The time series at the ocean and river points (lower panels of Figure 5) reflect this, with a maximum wave of almost 0.5 meters seen at point A, and the same peak showing up at point B a half hour later as a 0.2 meters wave. The time series shows that the models both predict the same timing for the initial wave. The forecast model tends to predict slightly higher wave magnitudes than the reference model.

The next event shown, caused by the 1994 Kuril earthquake (Figure 6), is of a smaller magnitude. The maximum wave amplitude maps differ in that the forecast model shows a

higher wave north of the breakwater, while the reference model predicts a high to the south. But the wave heights in the river channel are matched. Looking at the time-series at point the ocean point A, the traces are well paired, suggesting that the differences in wave heights between the models are limited to nearer the coast.

The 1996 Andreanof, 2001 Peru, 2003 Rat Island, and 2006 Tonga events (Figures 7-10) events result in smaller wave heights at Florence, and the models show a very good correlation of wave height predictions. The maximum waves seen at the time series points are all less than 5 cms, and the forecast and reference models show very good agreement in their predictions of magnitude and timing of the tsunami waves.

The two Kuril events, from 2006 and 2007 (Figures 11 and 12) are moderate. The 2006 maximum wave heights correlate well, with the reference model predicting slightly higher near-shore waves south of the breakwater. The time series for both these events show good agreement in timing and magnitude, but the forecast model tends to predict slightly higher waves/

The last three events shown, the 2007 Solomon, Peru and Chile events (Figures 13-15) are all smaller events. The Chile and Peru events show maximum wave heights that do not break 2 centimeters. The Solomon event is slightly larger and is unique in its lower frequency waves. The forecast model predicts results very similar to the reference model for each event.

3.2 Model stability and reliability

Recorded historical tsunamis provide only a limited number of events, from limited locations. More comprehensive test cases of destructive tsunamis with different directionalities are needed to check the stability and robustness of the tsunami forecast models. To this end, a subset of 16 synthetic M_w 9.3 tsunamis as in Tang *et al.* (2008) was selected for further examination. The sources used as input to the computational grids are from the propagation database developed by NCTR (Gica *et al.*, 2008). Table 4 lists the 16 synthetic tsunami events used here and their unit source combinations. The events are from sources spread around the Pacific,

The resulting modeled wave height signals from the developed forecast model are shown in Fig 16. These time-series are from the point offshore of the Florence dock, labeled as 'B' in the previous series of figures. The most severe wave height signal is caused by the S06_acsz scenario, a M_w 9.3 event on the nearby Cascadian subduction fault, with wave heights reaching 6 meters for this event. The S18_kisz scenario causes the second largest simulated waves seen at Florence, from an earthquake on the other side of the Pacific on the Kamchatka-Yap section. In contrast, mega-events that occur in Central and South America and the South Pacific result in smaller wave heights for Florence. Those, while still significant, are not as dramatic. Lastly, note that the tsunami forecast model developed for Florence is numerically stable for all these mega-events, and can withstand the very high energies released.

4.0 Summary and Conclusions

We have developed reference and forecast models for Florence, Oregon. The computational grids were derived from the best available bathymetric and topographic source data available. Testing and comparison was undertaken using eleven historical tsunami events. The forecast models were validated by comparing predicted wave heights and velocities with a higher resolution RIM model. In addition, the stability and sensitivity of the model were tested with 16 M_w 9.3 synthetic tsunami scenarios originating

around the Pacific Rim and South American coast. The forecast model remained stable during the synthetic testing. Scenarios run using Alaska-Cascadia and Kuril-Kamchatka sources would result in waves as high as 6 m in the Siuslaw River channel. The forecast model can provide a 4-hr forecast model of the first wave arrival, amplitudes, and inundation within 10 min of clock time.

5.0 Acknowledgments

I would like to thank Nazila Merati for editorial assistance in the writing of this report and Yong Wei for his assistance with model setup and troubleshooting. This publication is partially funded by the Joint Institute for the Study of the Atmosphere and Ocean (JISAO) under NOAA Cooperative Agreement No. NA17RJ1232, JISAO Contribution No. xxxx. This is PMEL Contribution No. XXXX.

6.0 References

Forthcoming

7.0 Appendix A

7.1 Reference model *.infile for Florence, Oregon

```
0.001 Minimum amplitude of input offshore wave (m) :
5      Input minimum depth for offshore (m)
0.1    Input "dry land" depth for inundation (m)
0.0009 Input friction coefficient (n**2)
1      let a and b run up
100.0   max eta before blow up (m)
.25     Input time step (sec)
144000  Input amount of steps
12      Compute "A" arrays every n-th time step, n=
6       Compute "B" arrays every n-th time step, n=
480     Input number of steps between snapshots
0       ...Starting from
1       ...Saving grid every n-th node, n=
```

7.2 Forecast model *.infile for Florence, Oregon

```
0.0001      Minimum amplitude of input offshore wave (m):
5          Input minimum depth for offshore (m)
0.1        Input "dry land" depth for inundation (m)
0.0009      Input friction coefficient (n**2)
1          let a and b run up
100.0       max eta before blow up (m)
1.2        Input time step (sec)
30000      Input amount of steps
5          Compute "A" arrays every n-th time step, n=
2          Compute "B" arrays every n-th time step, n=
100        Input number of steps between snapshots
0          ...Starting from
1          ...Saving grid every n-th node, n=
```


Table 1 NGDC run up observations for Florence, Oregon.

		Reference Model			Forecast Model		
Grid	Region	Coverage Lat (W) Long (N)	Cell size	Time Step [sec]	Coverage Long (W) Lat (N)	Cell Size	Time Step [sec]
A	Central Oregon and South West Washington	39.0 – 48.0 126.5 – 123.5	36		39.01 – 47.19 127.5 – 123.5	72	
B	Oregon Coast	43.5 – 44.5 124.8 - 124.0	6		43.5 – 44.5 124.8 - 124.0	12	
C	Florence	43.9580 – 44.0520 124.1900 – 124.0800	0.33	0.25	43.9580 – 44.0520 124.1900 – 124.0800	1.8	1.2
Minimum offshore depth (m)		5			5		
Water depth for dry land (m)		0.1			0.1		
Manning coefficient, n		0.0009			0.0009		
CPU time needed for a 4 hour simulation		7.5 hr			10.3 min		

Table 2 MOST Model set up parameters for Florence, Oregon

Event	Time (UTC)	Zone	Mw	Lon	Lat	Source
Chile	2007.11.14 15:40:52	SASZ	7.6	69.9W	22.2S	$0.81 \times a_{22} + 0.33 \times a_{23} + 0.11 \times b_{23}$
Peru	2007.08.15 23:40:57	SASZ	8.1	76.509W	13.354S	$4.3 \times a_9 + 4.1 \times b_9$
Solomon	2007.04.01 20:40:40.7	NBSV	8.2	156.4E	7.96S	$12.0 \times b_{10}$
Kuril	2007.01.13 04:23:48.2	KISZ	7.9	154.80E	46.18N	$-3.82 \times b_{13}$
Kuril	2006.11.15 11:14:16	KISZ	8.1	154.32E	46.75N	$4.0 \times a_{12} + 0.5 \times b_{12} + 2.0 \times a_{13} + 1.5 \times b_{13}$
Tonga	2006.05.03 15:26:39	NZKT	8.1	174.164W	20.13N	$8.44 \times b_{29}$
Rat Island	2003.11.17 06:43:07	AASZ	7.8	178.74E	51.13N	$2.81 \times b_{11}$
Peru	2001.06.23 20:33:14	SASZ	8.2	73.31W	16.14S	$5.7 \times a_{15} + 2.9 \times b_{16} + 1.98 \times a_{16}$
Andreanof	1996.06.10 04:03:35.4	AASZ	7.8	176.847E	51.478N	$2.4 \times a_{15} + 0.8 \times b_{16}$
Kuril	1994.10.04 13:22:58.3	KISZ	8.1	147.328E	43.706N	$9.0 \times a_{20}$
Unimak	1946.04.01 12:28:56	AASZ	8.1	163.19W	53.32	$7.5 \times b_{23} + 19.70 \times b_{24} + 3.7 \times b_{25}$

Table 3 Tsunami sources of 11 historical events used for model validation in this study.

Event	Source
S01_kisz_ab22T31	Kamchatka-Yap, Pacific grid: Mwt 9.3, 29.00*a22+29.00*b22+29.00*a23+29.00*b23+29.00*a24+29.00*b24+29.00*a25+29.00*b25+29.00*a26+29.00*b26+29.00*a27+29.00*b27+29.00*a28+29.00*b28+29.00*a29+29.00*b29+29.00*a30+29.00*b30+29.00*a31+29.00*b31
S02_kisz_ab1T10	Kamchatka-Yap, Pacific grid: Mwt 9.3, 29.00*a1+29.00*b1+29.00*a2+29.00*b2+29.00*a3+29.00*b3+29.00*a4+29.00*b4+29.00*a5+29.00*b5+29.00*a6+29.00*b6+29.00*a7+29.00*b7+29.00*a8+29.00*b8+29.00*a9+29.00*b9+29.00*a10+29.00*b10
S03_acsz_ab12T21	Aleutian-Cascadia, Pacific grid: Mwt 9.3, 29.00*a12+29.00*b12+29.00*a13+29.00*b13+29.00*a14+29.00*b14+29.00*a15+29.00*b15+29.00*a16+29.00*b16+29.00*a17+29.00*b17+29.00*a18+29.00*b18+29.00*a19+29.00*b19+29.00*a20+29.00*b20+29.00*a21+29.00*b21
S04_acsz_ab22T31	Aleutian-Cascadia, Pacific grid: Mwt 9.3, 29.00*a22+29.00*b22+29.00*a23+29.00*b23+29.00*a24+29.00*b24+29.00*a25+29.00*b25+29.00*a26+29.00*b26+29.00*a27+29.00*b27+29.00*a28+29.00*b28+29.00*a29+29.00*b29+29.00*a30+29.00*b30+29.00*a31+29.00*b31
S05_acsz_ab38T47	Aleutian-Cascadia, Pacific grid: Mwt 9.3, 29.00*a38+29.00*b38+29.00*a39+29.00*b39+29.00*a40+29.00*b40+29.00*a41+29.00*b41+29.00*a42+29.00*b42+29.00*a43+29.00*b43+29.00*a44+29.00*b44+29.00*a45+29.00*b45+29.00*a46+29.00*b46+29.00*a47+29.00*b47
S06_acsz_ab56T65	Aleutian-Cascadia, Pacific grid: Mwt 9.3, 29.00*a56+29.00*b56+29.00*a57+29.00*b57+29.00*a58+29.00*b58+29.00*a59+29.00*b59+29.00*a60+29.00*b60+29.00*a61+29.00*b61+29.00*a62+29.00*b62+29.00*a63+29.00*b63+29.00*a64+29.00*b64+29.00*a65+29.00*b65
S07_sasz_ab1T10	Central America, Pacific grid: Mwt 9.3, 29.00*a1+29.00*b1+29.00*a2+29.00*b2+29.00*a3+29.00*b3+29.00*a4+29.00*b4+29.00*a5+29.00*b5+29.00*a6+29.00*b6+29.00*a7+29.00*b7+29.00*a8+29.00*b8+29.00*a9+29.00*b9+29.00*a10+29.00*b10
S09_sasz_ab40T49	South American, Pacific grid: Mwt 9.3, 29.00*a40+29.00*b40+29.00*a41+29.00*b41+29.00*a42+29.00*b42+29.00*a43+29.00*b43+29.00*a44+29.00*b44+29.00*a45+29.00*b45+29.00*a46+29.00*b46+29.00*a47+29.00*b47+29.00*a48+29.00*b48+29.00*a49+29.00*b49
S11_ntsz_ab20T29	New Zealand-Kermadec-Tonga, Pacific grid: Mwt 9.3, 29.00*a20+29.00*b20+29.00*a21+29.00*b21+29.00*a22+29.00*b22+29.00*a23+29.00*b23+29.00*a24+29.00*b24+29.00*a25+29.00*b25+29.00*a26+29.00*b26+29.00*a27+29.00*b27+29.00*a28+29.00*b28+29.00*a29+29.00*b29
S12_ntsz_ab30T39	New Zealand-Kermadec-Tonga, Pacific grid: Mwt 9.3, 29.00*a30+29.00*b30+29.00*a31+29.00*b31+29.00*a32+29.00*b32+29.00*a33+29.00*b33+29.00*a34+29.00*b34+29.00*a35+29.00*b35+29.00*a36+29.00*b36+29.00*a37+29.00*b37+29.00*a38+29.00*b38+29.00*a39+29.00*b39

S13_nvsz_ab28T37	New Britain-Solomons-Vanuatu, Pacific grid: Mwt 9.3, 29.00*a28+29.00*b28+29.00*a29+29.00*b29+29.00*a30+29.00*b30+29.00*a31+29.00*b31+29.00*a32+29.00*b32+29.00*a33+29.00*b33+29.00*a34+29.00*b34+29.00*a35+29.00*b35+29.00*a36+29.00*b36+29.00*a37+29.00*b37
S14_mosz_ab1T10	Manus OCB, Pacific grid: Mwt 9.3, 29.00*a1+29.00*b1+29.00*a2+29.00*b2+29.00*a3+29.00*b3+29.00*a4+29.00*b4+29.00*a5+29.00*b5+29.00*a6+29.00*b6+29.00*a7+29.00*b7+29.00*a8+29.00*b8+29.00*a9+29.00*b9+29.00*a10+29.00*b10
S15_ngsz_ab3T12	North New Guinea, Pacific grid: Mwt 9.3, 29.00*a3+29.00*b3+29.00*a4+29.00*b4+29.00*a5+29.00*b5+29.00*a6+29.00*b6+29.00*a7+29.00*b7+29.00*a8+29.00*b8+29.00*a9+29.00*b9+29.00*a10+29.00*b10+29.00*a11+29.00*b11+29.00*a12+29.00*b12
S16_epsz_ab6T15	East Philippines, Pacific grid: Mwt 9.3, 29.00*a6+29.00*b6+29.00*a7+29.00*b7+29.00*a8+29.00*b8+29.00*a9+29.00*b9+29.00*a10+29.00*b10+29.00*a11+29.00*b11+29.00*a12+29.00*b12+29.00*a13+29.00*b13+29.00*a14+29.00*b14+29.00*a15+29.00*b15
S17_rnsz_ab12T21	Ryukus-Kyushu-Nankai, Pacific grid: Mwt 9.3, 29.00*a12+29.00*b12+29.00*a13+29.00*b13+29.00*a14+29.00*b14+29.00*a15+29.00*b15+29.00*a16+29.00*b16+29.00*a17+29.00*b17+29.00*a18+29.00*b18+29.00*a19+29.00*b19+29.00*a20+29.00*b20+29.00*a21+29.00*b21
S18_kisz_ab32T41	Kamchatka-Yap, Pacific grid: Mwt 9.3, 29.00*a32+29.00*b32+29.00*a33+29.00*b33+29.00*a34+29.00*b34+29.00*a35+29.00*b35+29.00*a36+29.00*b36+29.00*a37+29.00*b37+29.00*a38+29.00*b38+29.00*a39+29.00*b39+29.00*a40+29.00*b40+29.00*a41+29.00*b41

Table 4. Unit source combinations used for the 16 artificial mega-events.



Figure 1 Evacuation map for Florence, Oregon developed by the Oregon Department of Geology and Mineral Industries in consultation with local officials. It is intended to represent a worst-case scenario for a tsunami caused by an undersea earthquake near the Oregon coast. Evacuation routes were developed by local officials and reviewed by the Oregon Department of Emergency Management.

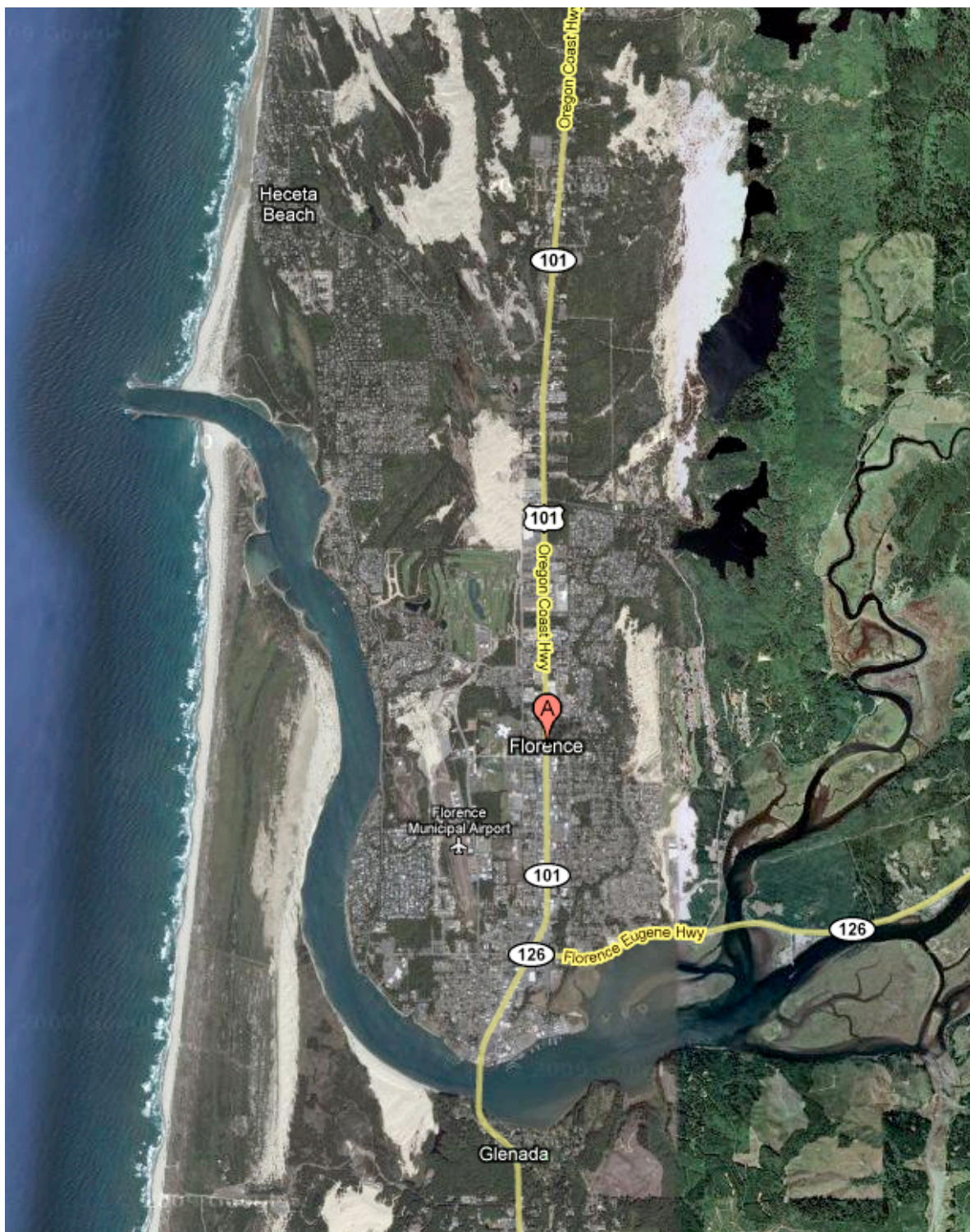


Figure 2 Google Maps image of Florence.

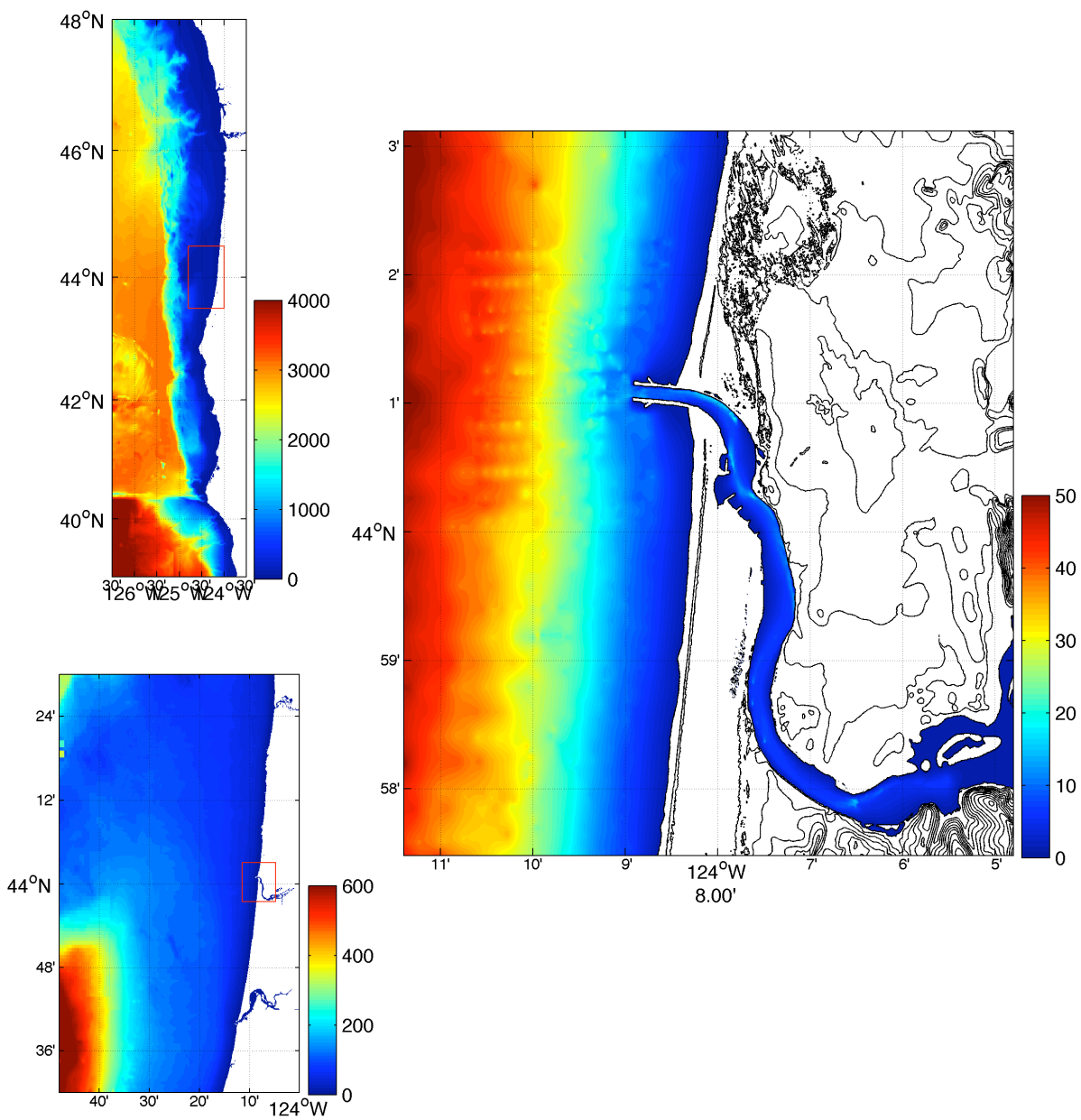


Figure 3 Bathymetry (in meters) for the Florence reference model grids. The A grid is shown in the top left axis, the B grid in the bottom left, and the C grid on the right. The land topography of the C grid is shown using contours with 10 meter intervals. The red boxes in the A and B plots show the position of the B and C grids, respectively.

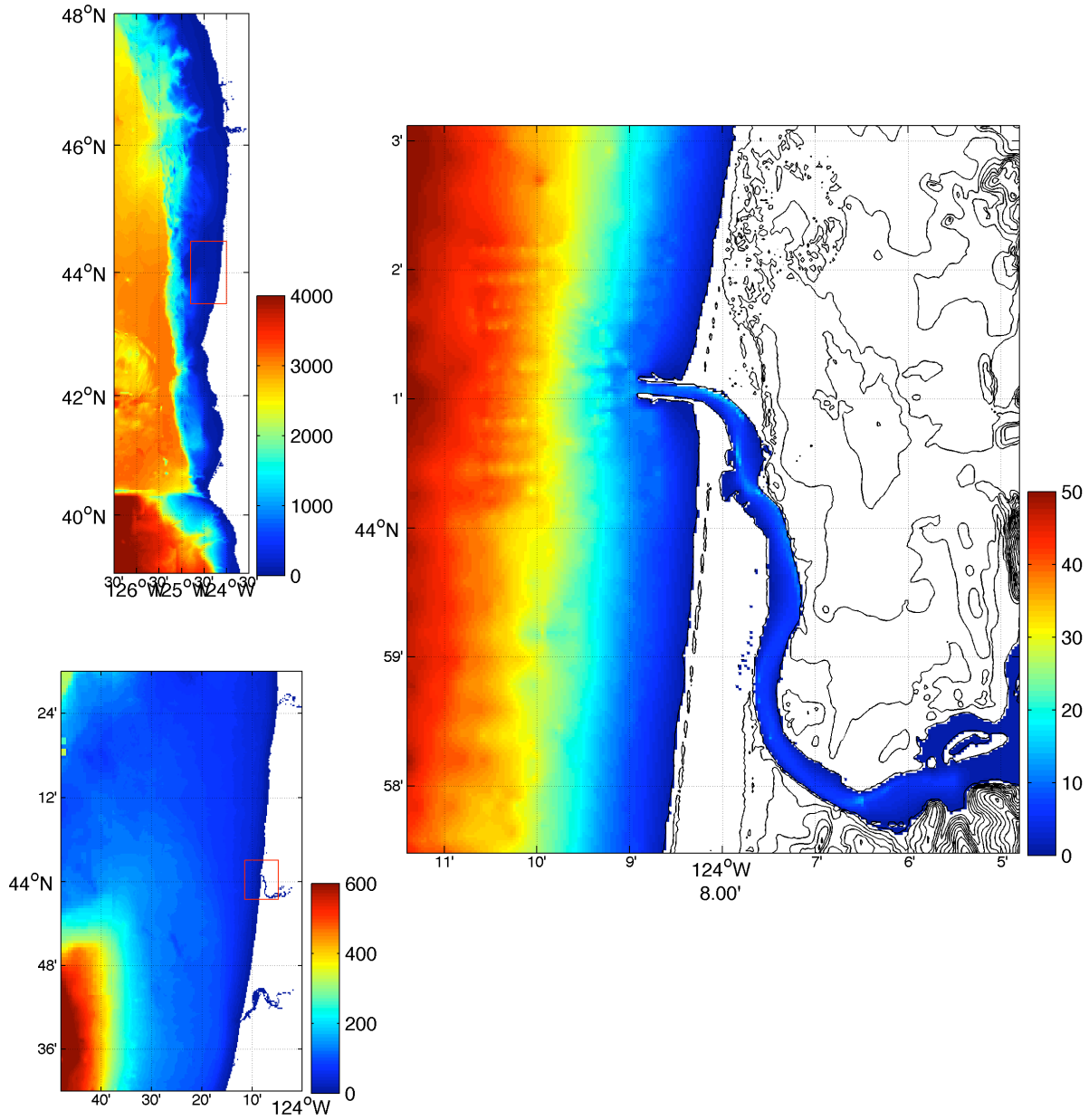
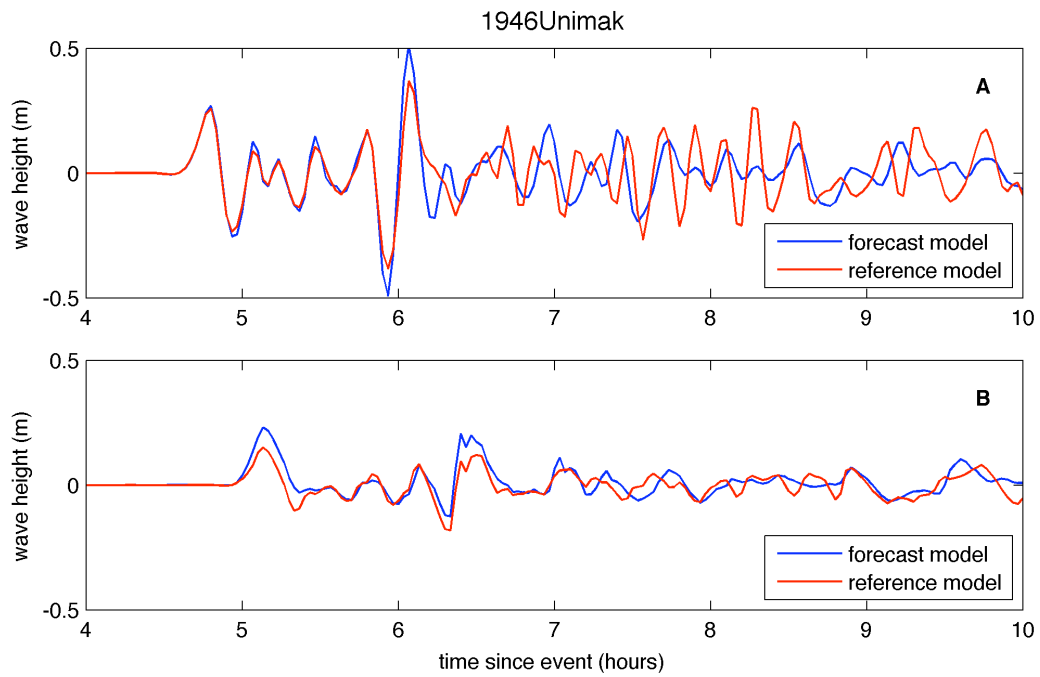
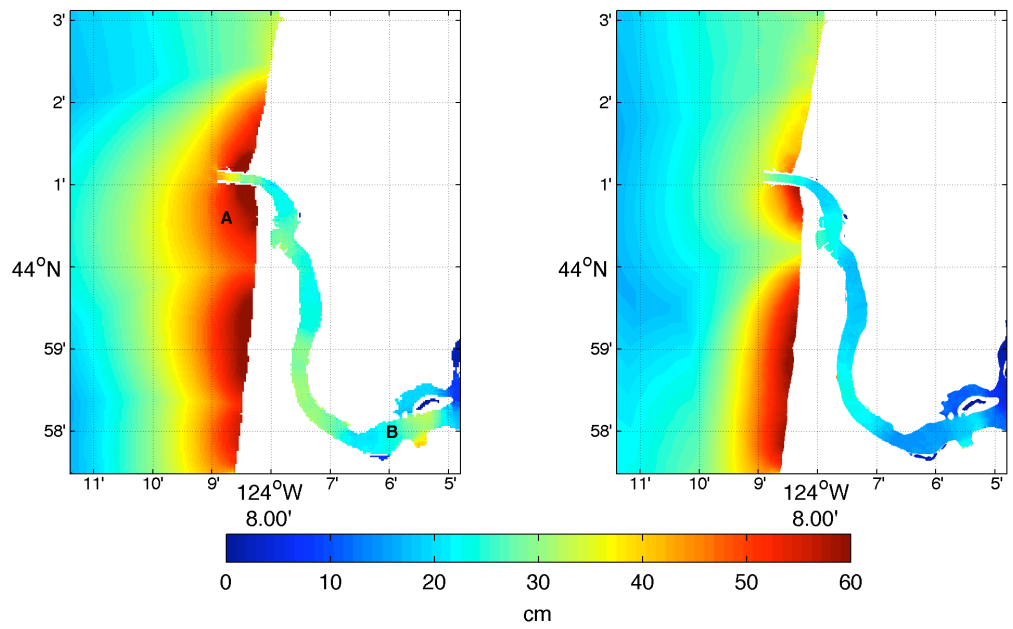


Figure 4 Bathymetry (in meters) for the Florence forecast model grids. The A grid is shown in the top left axis, the B grid in the bottom left, and the C grid on the right. The land topography of the C grid is shown using contours with 10 meter intervals. The red boxes in the A and B plots show the position of the B and C grids, respectively.



reference model maximum wave height results. The lower axes show the model wave height time-series at the A and B points shown in the upper left figure.

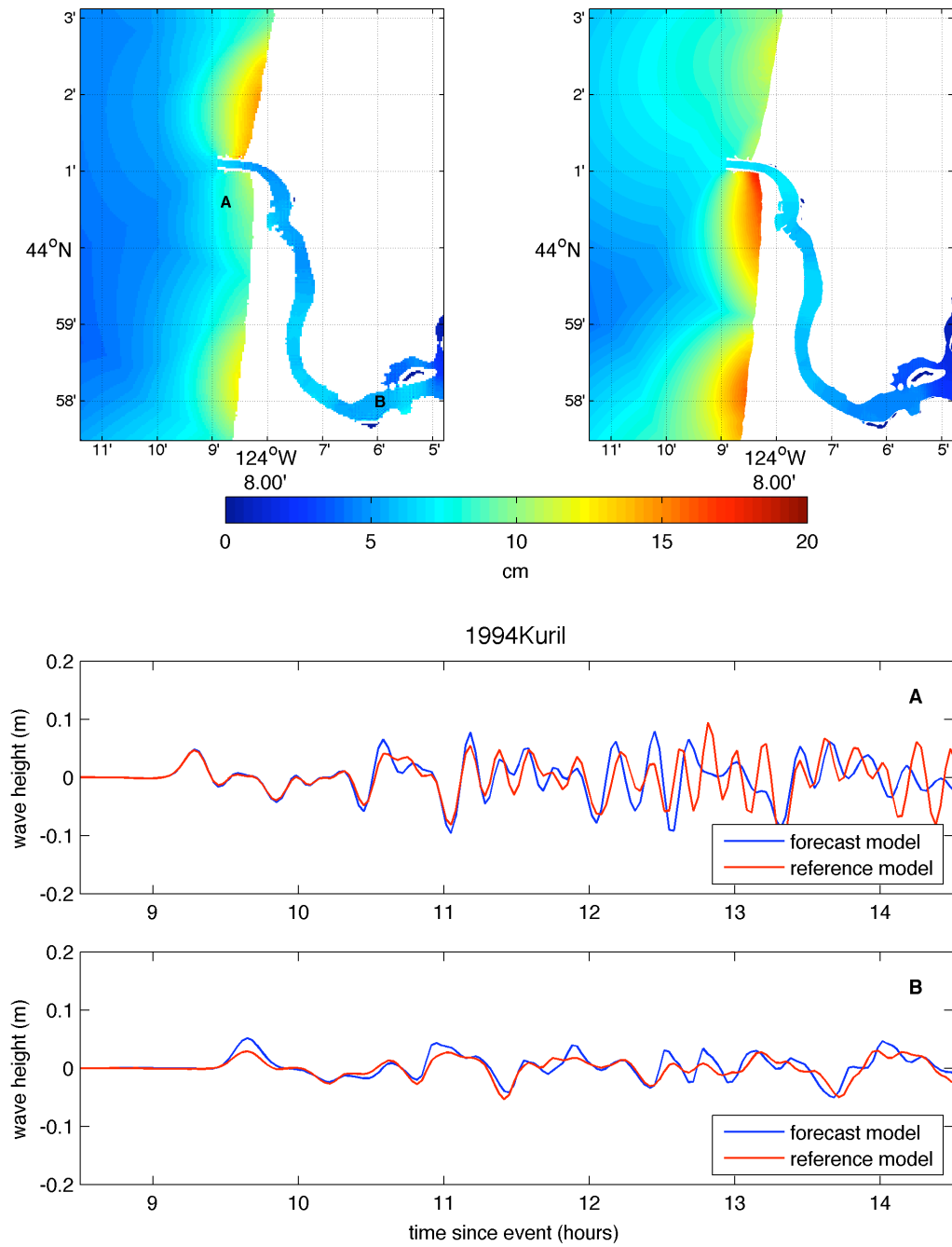


Figure 6 Model results for the 1994 Kuril event. Top left and right axes show, respectively, the forecast and reference model maximum wave height results. The lower axes show the model wave height time-series at the A and B points shown in the upper left figure.

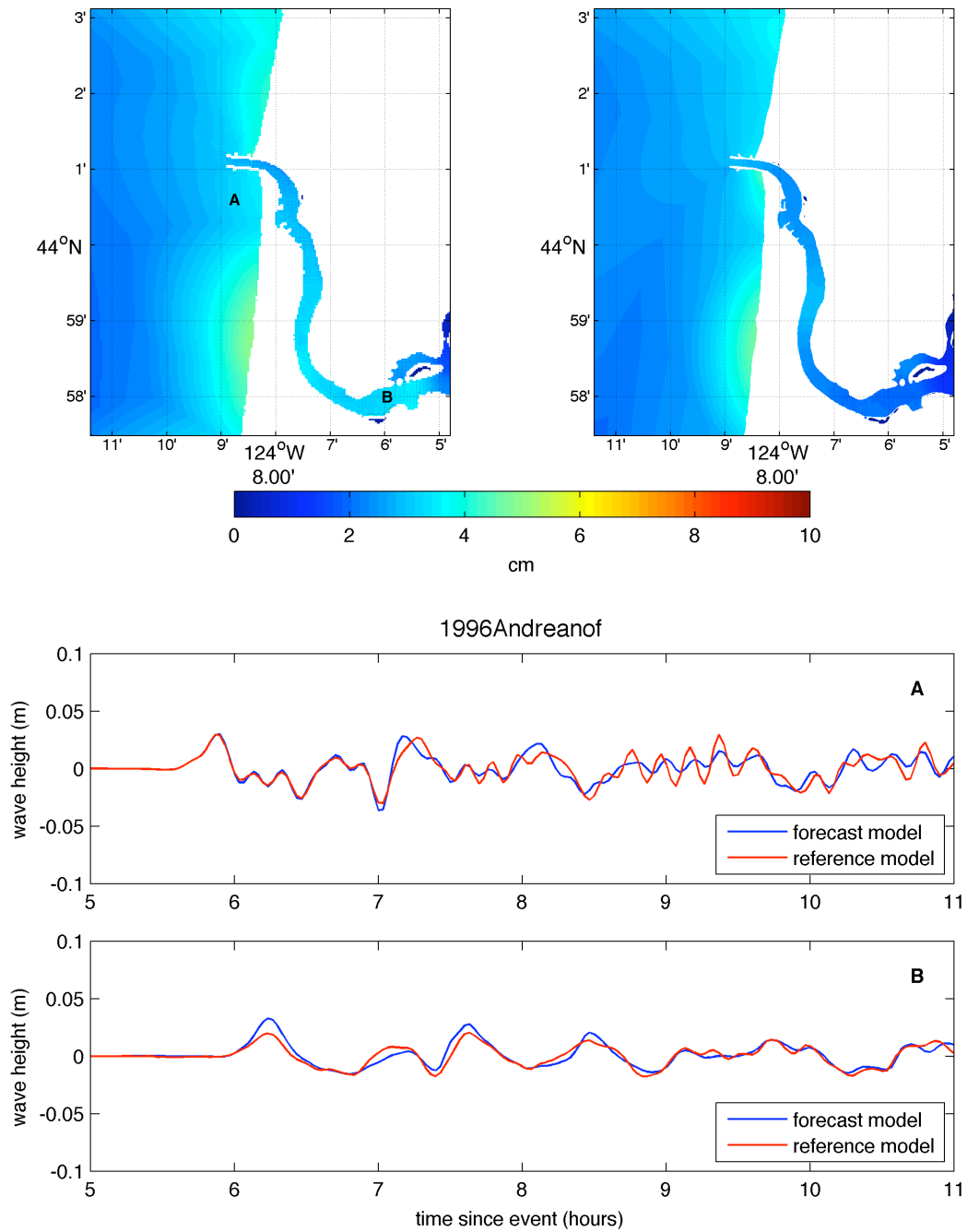


Figure 7 Model results for the 1996 Andreanof event. Top left and right axes show, respectively, the forecast and reference model maximum wave height results. The lower axes show a time-series of the model wave heights at the A and B points shown in the upper left figure.

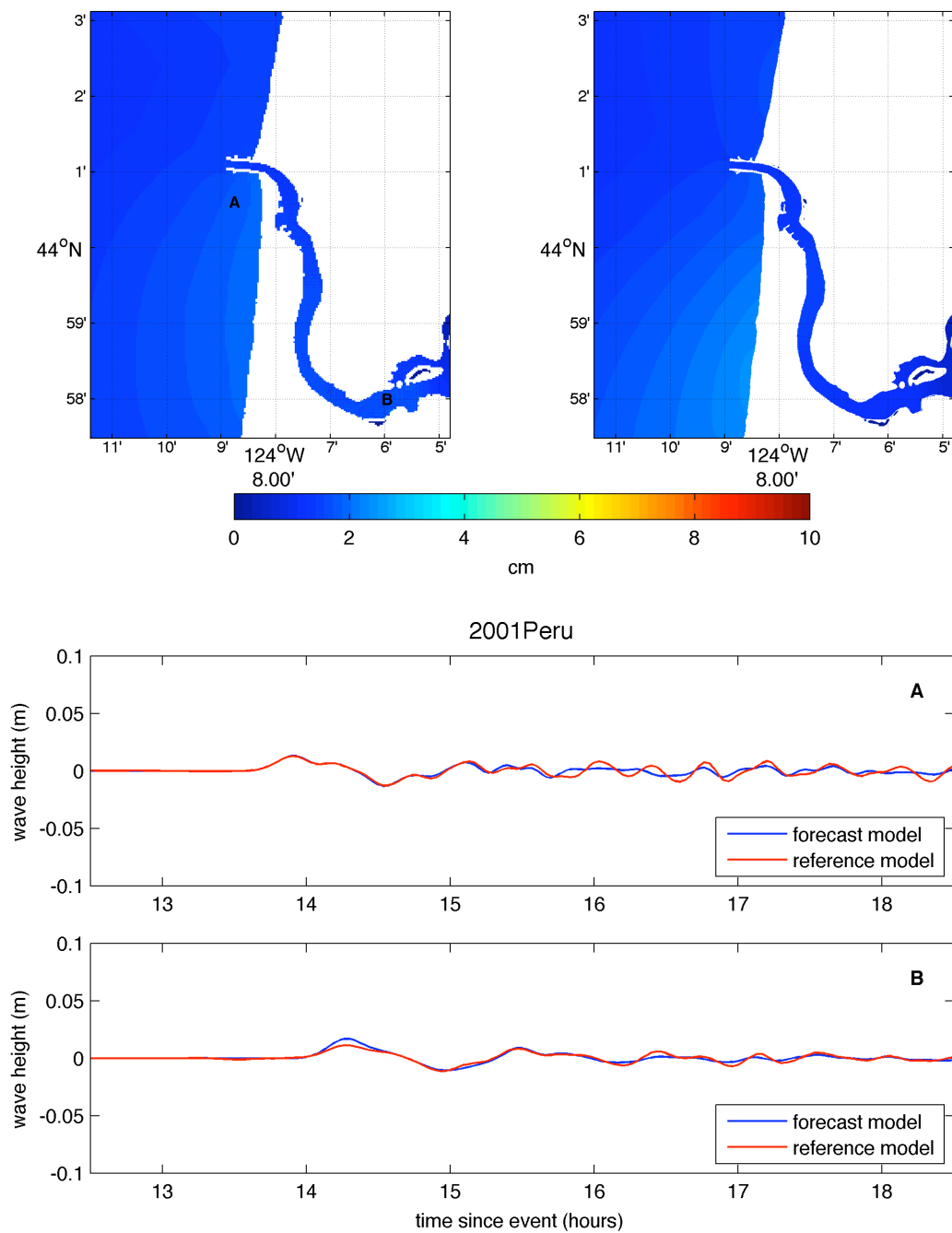


Figure 8 Model results for the 2001 Peru event. Top left and right axes show, respectively, the forecast and reference model maximum wave height results. The lower axes show the model wave height time-series at the A and B points shown in the upper left figure.

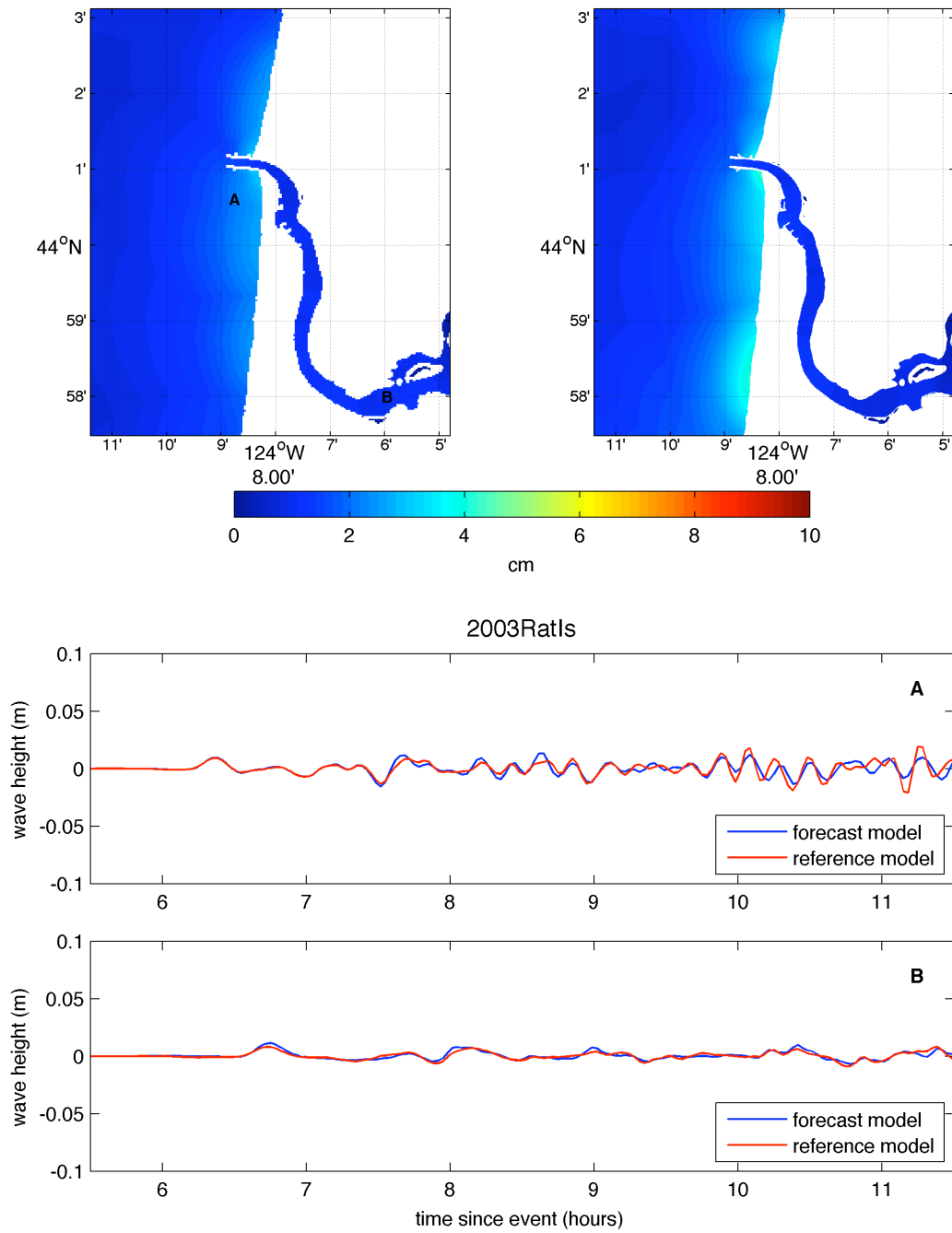


Figure 9 Model results for the 2003 Rat Island event. Top left and right axes show, respectively, the forecast and reference model maximum wave height results. The lower axes show the model wave height time-series at the A and B points shown in the upper left figure.

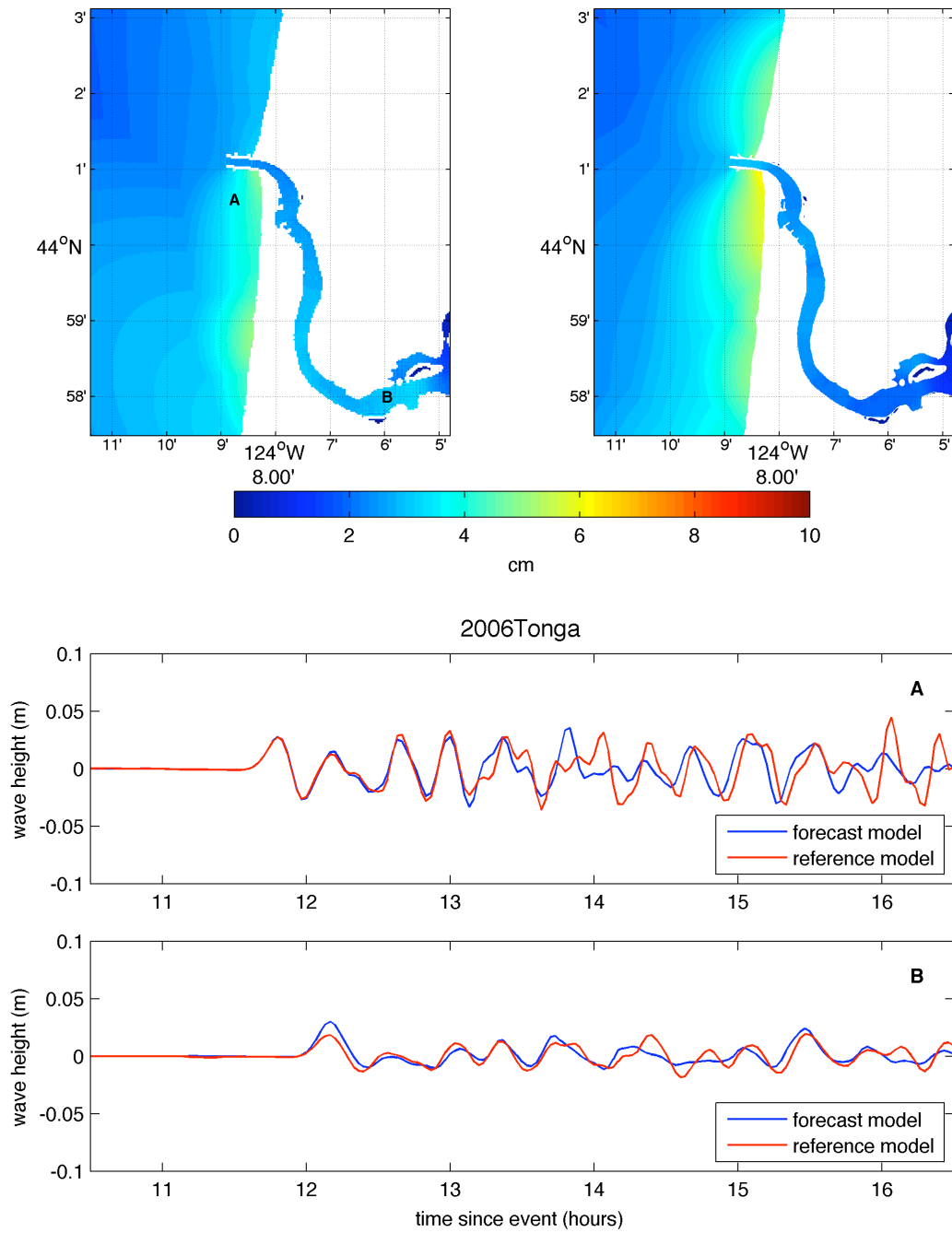
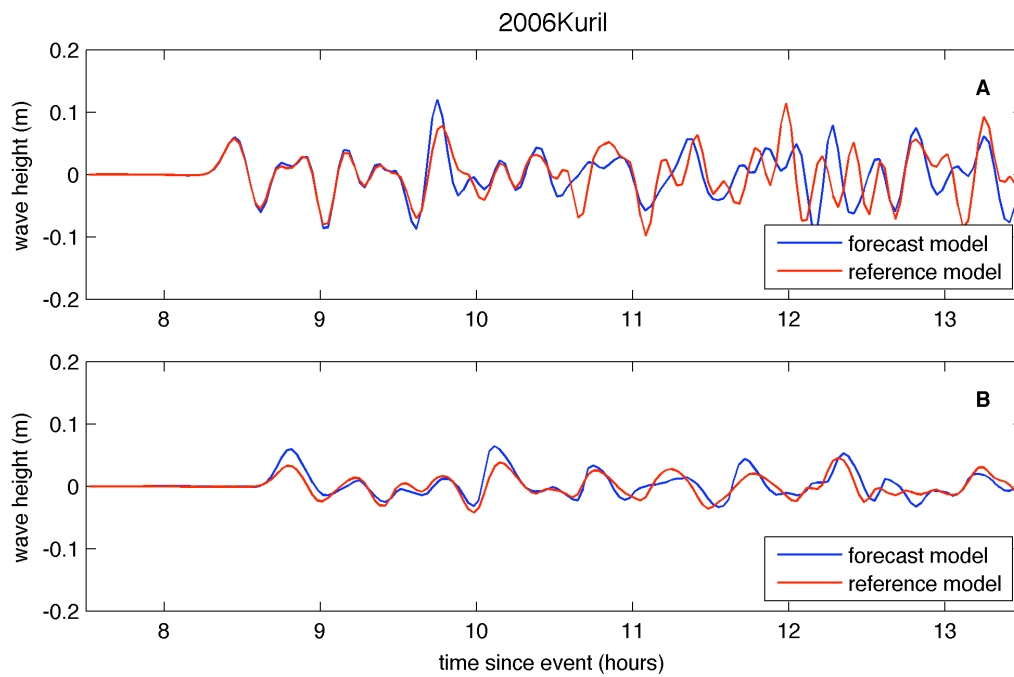
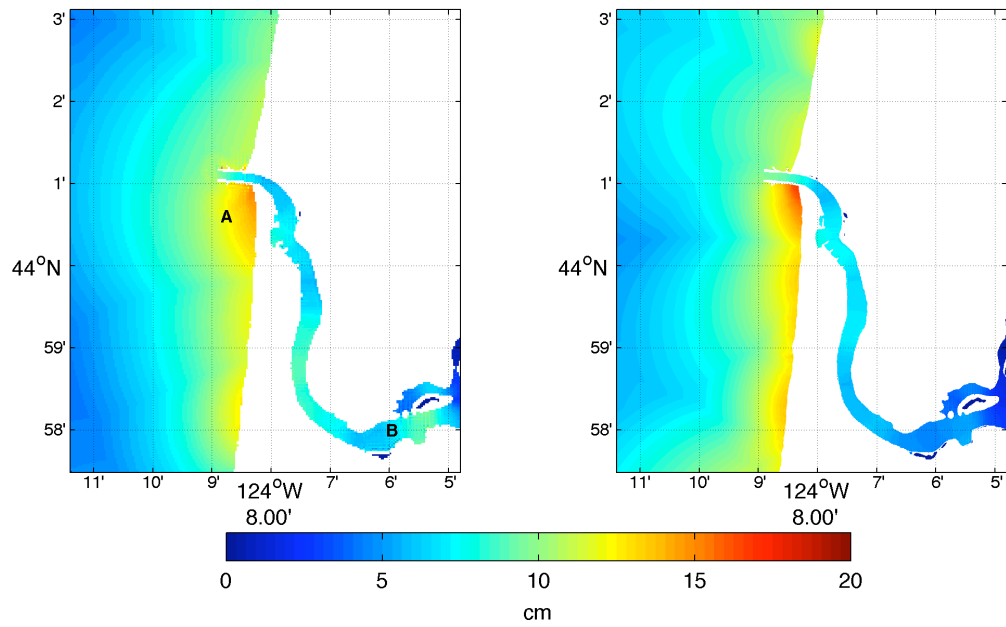


Figure 10 Model results for the 2006 Tonga event. Top left and right axes show, respectively, the forecast and reference model maximum wave height results. The lower axes show the model wave height time-series at the A and B points shown in the upper left figure.



I reference model maximum wave height results. The lower axes show the model wave height time-series at the A and B points shown in the upper left figure.

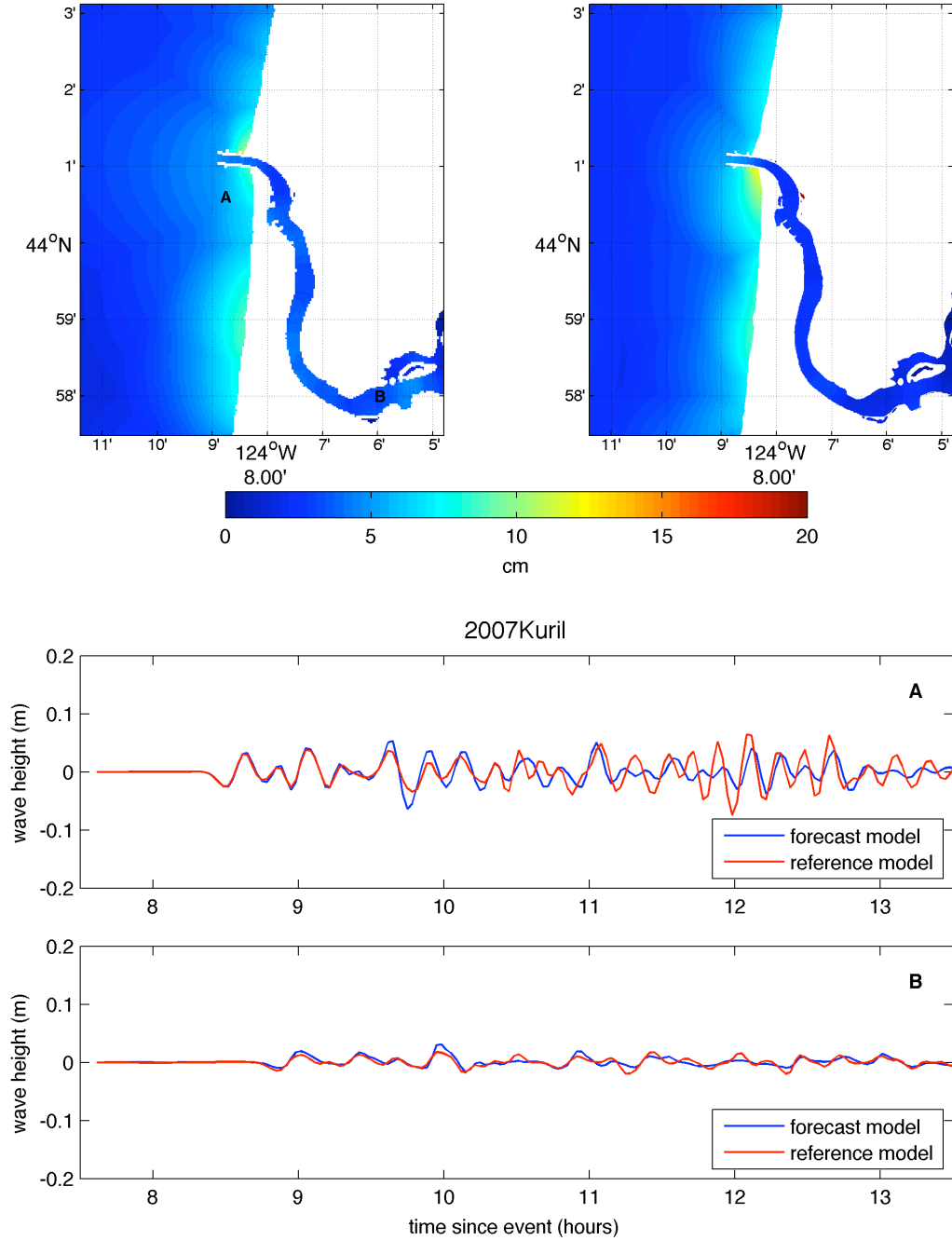


Figure 12 Model results for the 2007 Kuril event. Top left and right axes show, respectively, the forecast and reference model maximum wave height results. The lower axes show the model wave height time-series at the A and B points shown in the upper left figure.

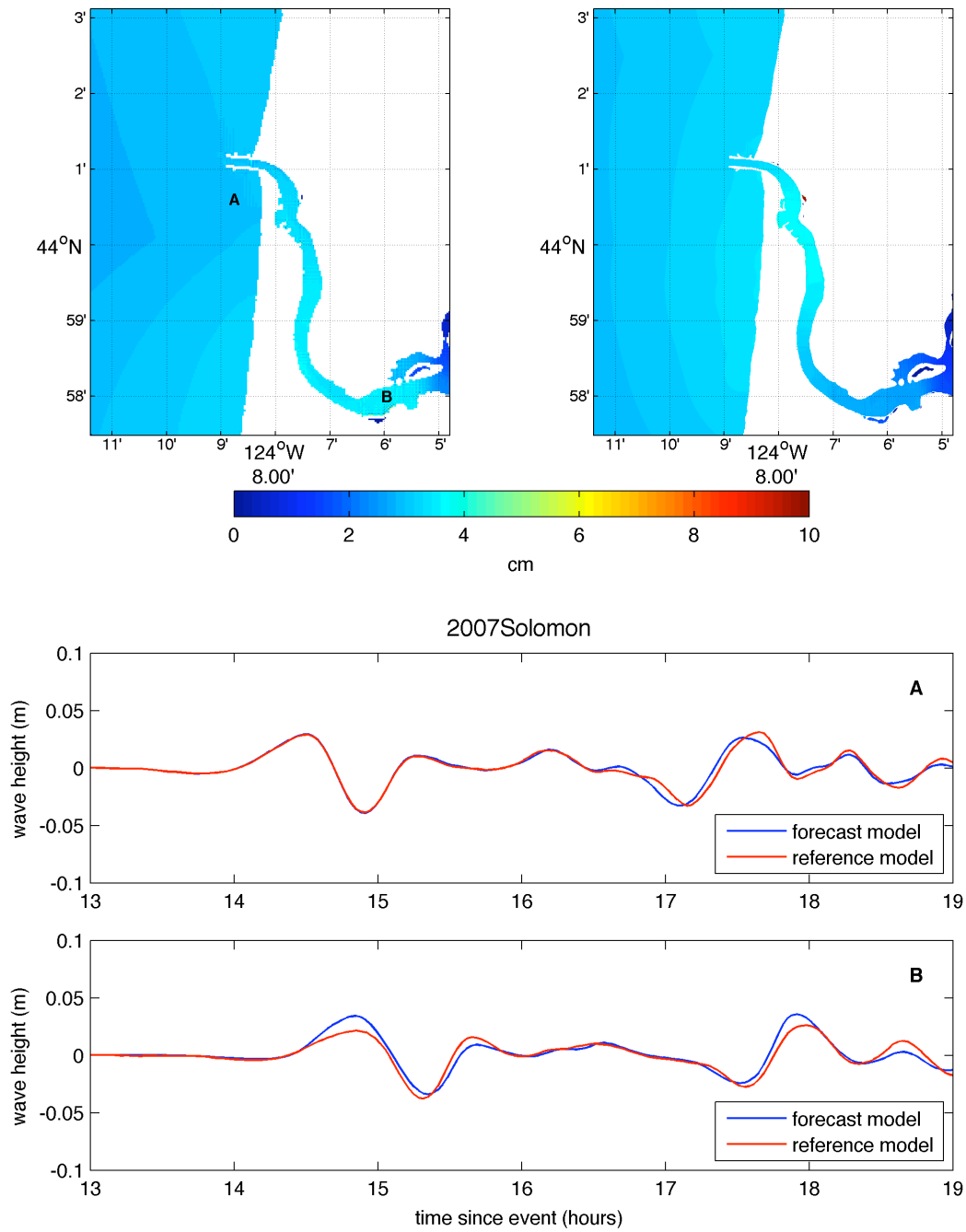


Figure 13 Model results for the 2007 Solomon Islands event. Top left and right axes show, respectively, the forecast and reference model maximum wave height results. The lower axes show the model wave height time-series at the A and B points shown in the upper left figure.

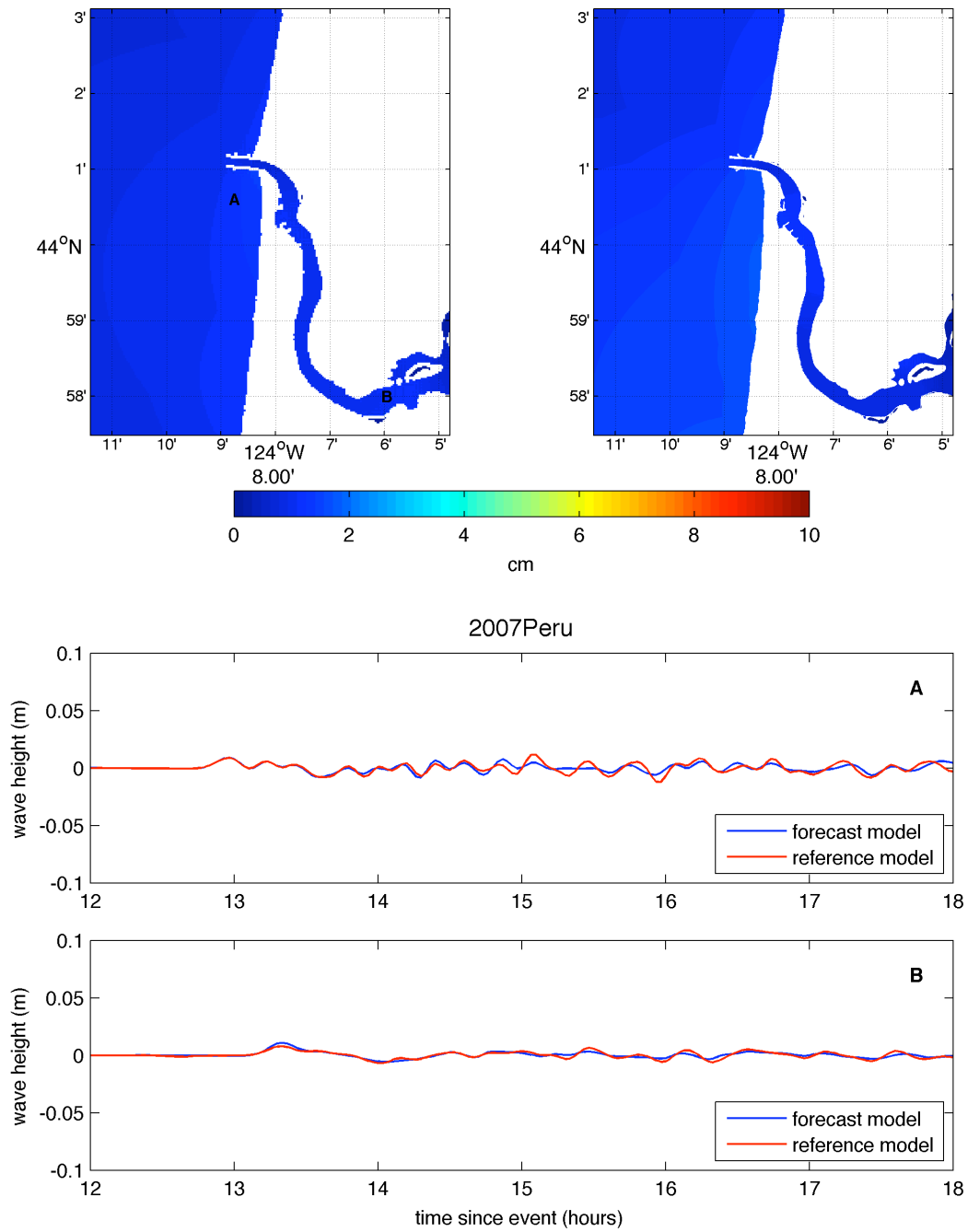


Figure 14 Model results for the 2007 Peru event. Top left and right axes show, respectively, the forecast and reference model maximum wave height results. The lower axes show the model wave height time-series at the A and B points shown in the upper left figure.

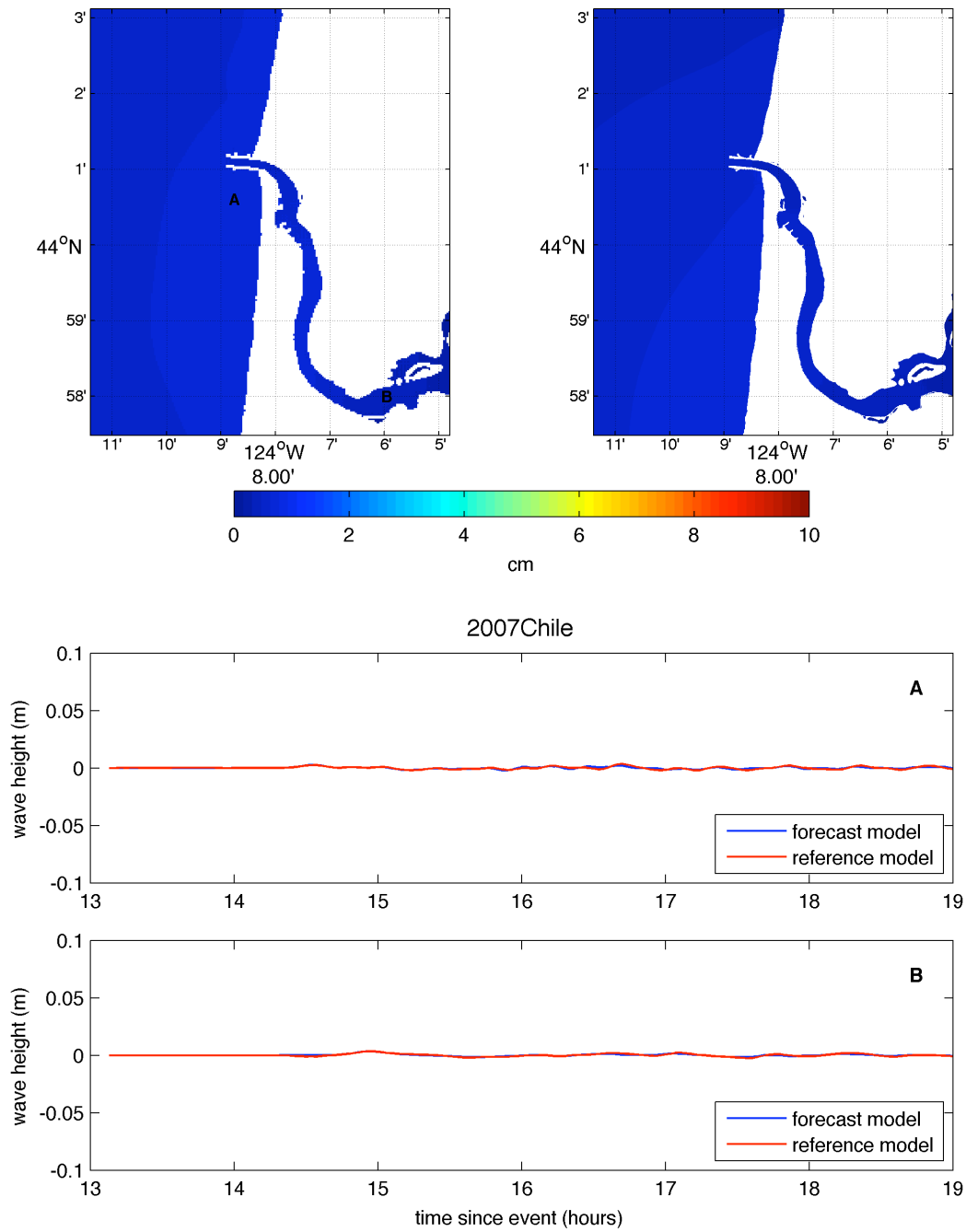


Figure 15 Model results for the 2007 Chile event. Top left and right axes show, respectively, the forecast and reference model maximum wave height results. The lower axes show the model wave height time-series at the A and B points shown in the upper left figure.

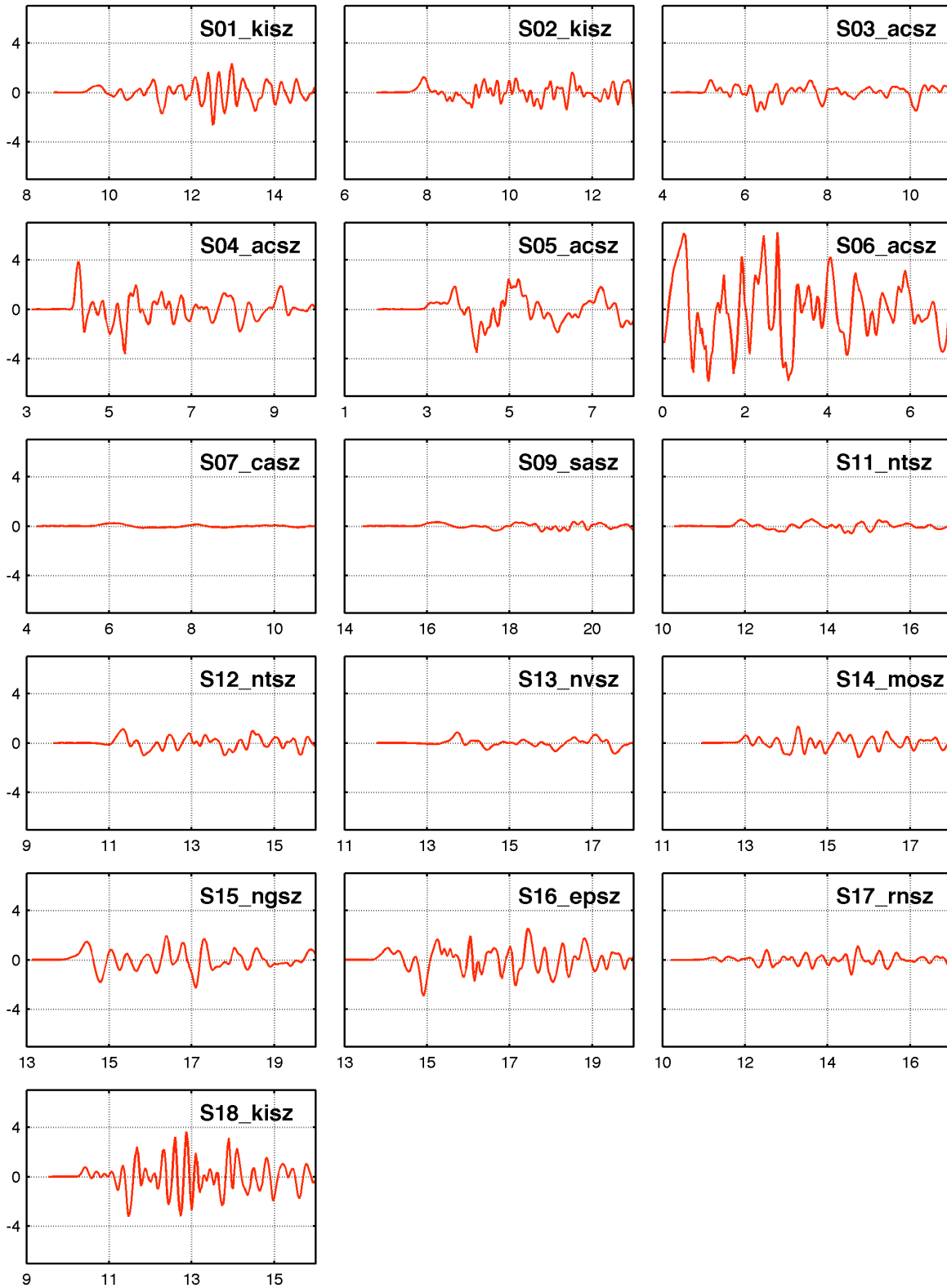


Figure 16 Wave heights (in meters) from the tsunami forecast model for 16 hypothetical mega-tsunami

scenarios. Time series are taken from a model point offshore of the Florence dock (the 'B' point in the previous figures). The x-axis units are hours since the event earthquake.